Effects of hot-rolling reduction on microstructure, texture and magnetic properties of high silicon steel produced by strip casting

D Y Hou, H J Xu, H T Jiao, C W Zhao, W Xiong, J P Yang, W Z Qiu and Y B Xu[1]

State Key Laboratory of Rolling and Automation, Northeastern University, Shenyang 110819, China

E-mail: yunbo_xu@126.com

Abstract. Non-oriented Fe-7.1wt.% Si as-cast strips were produced by twin-roll strip casting process. Then the as-cast strips were hot rolled with different reductions, followed by warm rolling and final annealing. The microstructure, texture evolution and magnetic properties were investigated in detail. The texture of hot rolled sheets with 40% reduction showed strongest {001}<110> texture, whereas the dominated texture was turned into {110}<001> and {110}<112>as the reduction was increased to 56% and 68%. After warm rolling and annealing, the average grain size was decreased firstly and then increased with an increase in hot rolling reduction. In the case of 40% hot rolling reduction, the recrystallization texture was dominated by strong γ (<111>//ND) texture. With an increase in hot rolling reduction, the γ texture was gradually weakened while α (<110>//RD) texture was enhanced. In addition, relatively stronger {100} texture was presented in the sheet of 68% hot rolling reduction. The highest B_{50} value attained was 1.66 T and the lowest $P_{10/400}$ was 24.26 W/kg at a reduction of 56%.

1. Introduction

High silicon electrical steels with high resistivity and almost zero magnetostriction are excellent soft magnetic materials for high-frequency motors, transformers, and magnetic shields [Refs]. However, it is extremely hard to produce high silicon steel by conventional rolling process because of the decreasing workability with the increase of silicon content. In order to overcome the poor workability, several methods have been proposed, such as rapid quenching [1], rapid solidification [2], spray forming [3], chemical vapor deposition (CVD) [4] and strip casting [5]. The only successful commercial manufacturing process is CVD technology developed by NKK Corp. In addition, the twin-roll strip casting (TRSC) technology is another promising alternate, which produces thin sheet directly from molten steel.

Extensive researches on the strip casting high silicon steel had been carried out [6-11]. Li [6] et al. investigated the microstructure and texture evolution along the whole processing routes. The beneficial recrystallization textures were formed in the products, such as {001}<210>, {001}<010>, {115}<5 10 1> and {410} <001>. Liu [7-8] et al. reported the properties of strip casting high silicon steels with different forming routes, and the microstructure, texture, formability and magnetic properties of the as-cast strips were studied in detail in the research. In addition, the properties of the alloy doped with cerium, the effects of warm-rolling temperature, and the tensile properties of the sheets rolled at elevated temperatures were also investigated [9-11]. Although TRSC has mostly

solved the problem of workability, the brittleness is still an obstacle for industrialization of high silicon steels. Hot rolling process is an important procedure to reduce the thickness of sheet. While, different processes may have different effects on the microstructure and texture. Thus, the further study on the hot rolling process in high silicon manufacture is necessary.

In the present work, high silicon as-cast strips were produced by twin-roll strip casting and followed by different hot rolling processes. Then the hot-rolled sheets were warm-rolled and annealed. The effects of rolling reduction on the evolution of microstructure, texture and magnetic properties were investigated.

2. Experimental procedures

The chemical composition of the alloyed strip was examined with Optima 8300DV inductively coupled plasma-atomic emission spectrometer (Table 1.). The as-cast strips with 140 mm width and 2.5 mm thickness were fabricated by a vertical type twin-roll strip caster. The as-cast strips were hot rolled to 1.5 mm, 1.1 mm and 0.8 mm at 1050℃ respectively. Then the sheets were warm-rolled to 0.5 mm at 650 ℃. After that, all the rolled sheets were finally annealed at 1050℃ for 5 min.

Table 1. Chemical composition of the as-cast strip (mass fraction, %)

C	Si	Al	Mn	S
0.005	7.09	0.11	0.23	0.016

The microstructures of the as-cast, rolled and annealed sheets were characterized by metallographic investigations. Textures were quantitatively examined with $Co_{K\alpha1}$ radiation in the Bruker D8 Discover X-ray diffraction (XRD). Electron backscattered diffraction (EBSD) analysis was partly performed to investigate the microstructure and micro-texture of hot-rolled samples on the FEI Quanta 600 scanning electron microscopy (SEM). Results of the texture measurements were presented in the form of Orientation Distribution Function (ODF). The magnetic inductions at 800 Am^{-1} (B_8), 5000 Am^{-1} (B_{50}) and the iron losses at 50 Hz and 1.5 T ($P_{15/50}$), 400 Hz and 1 T ($P_{10/400}$), were respectively measured using a single sheet tester in both rolling and transverse directions of the annealed specimens with 100 mm length and 30 mm width.

3. Results and discussion

3.1. Microstructure and texture of the as-cast strip

Figure 1 shows the microstructure and texture of the as-cast strip. The microstructure of as-cast strip was consisted of some fine columnar grains at the subsurface layer and coarser equiaxed grains at the center layer (Figure 1a). The average grain size was 134 μm. The texture of as-cast strip was characterized by pronounced λ-fiber (<100>//ND) texture and weak α-fiber texture, as show in Figure 1b and c.

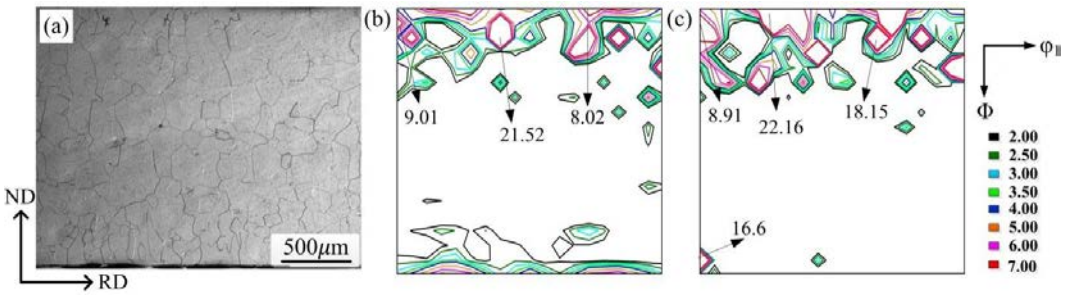

Figure 1. Microstructure (a) and ODF ((b) φ_2=0°, (c) φ_2=45°) of the as-cast strip.

3.2. Microstructure and texture of the hot rolled sheets

Figure 2 presents the microstructure of the hot rolled sheets. With the increase of the hot-rolling reduction, the average grain size increased gradually. The large grains in sample of 56% and 68% reduction were induced by the heat treatment during rolling passes. Figure 3 shows the texture of the hot rolled sheets. The hot rolling reduction had a significant influence on the texture evolution. The texture of the sheets with 40 % reduction was similar to the initial as-cast strip, which were characterized by strong {001}<110> and weak {001}<100> texture, as shown in Figure 3a. When the hot rolling reduction increased from 56% to 68%, λ-fibre texture almost disappeared, replaced by strong Goss ({110} <001>) and Brass ({110}<112>) texture respectively. In addition, the intensity of α-fiber texture increased firstly and then decreased slightly, as shown in Figure 3b and c.

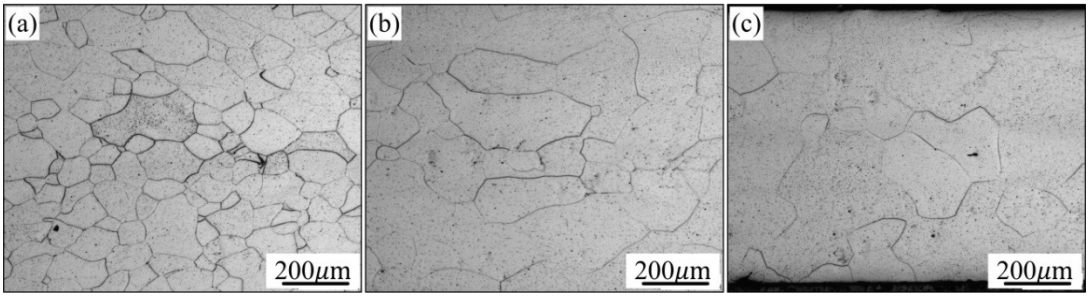

Figure 2. Microstructure of hot rolled sheets with reductions of: (a) 40%; (b) 56%; (c) 68%.

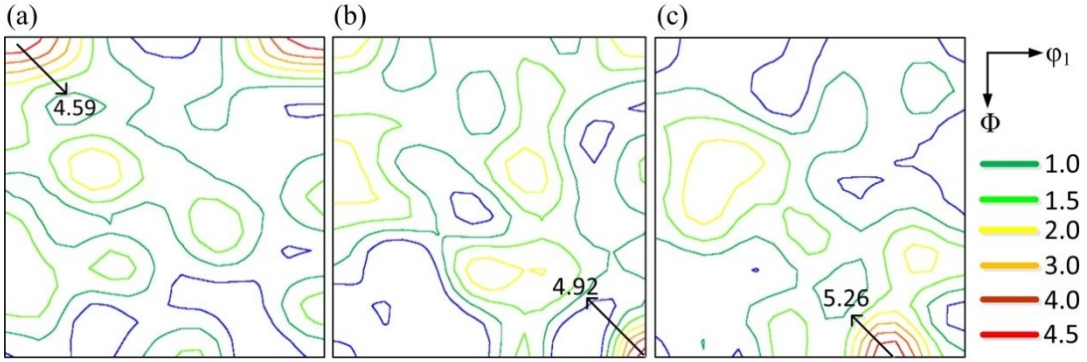

Figure 3. ODF (φ_2=45°) of hot rolled sheets with reductions of: (a) 40%; (b) 56%; (c) 68%.

3.3. Microstructure and texture of the warm-rolled sheets

Figure 4 shows the microstructure of the warm-rolled sheets. It was clearly found that the microstructure evolution highly depended on the rolling reduction. The shape of grains was the obvious elongated grains along the rolling direction. Some grains went through the whole visual field. As the hot rolling reduction of increased, the elongation of grains was more evident, and the average grain size was increased from 97.3 μm to 178.4 μm. Evident in-grain shear bands were not observed because the warm-rolling was carried out by multiple passes with small reduction and heat preservation for 4 min between passes. Figure 5 shows the texture of the warm-rolled sheets. The warm-rolled texture was characterized by strong γ-fiber (<111>//ND) texture, λ-fiber and weak α-fiber component. As the increase in hot rolling reduction, the intensity of γ-fiber texture was increased firstly and then decreased. While, the {100} texture was weakened gradually.

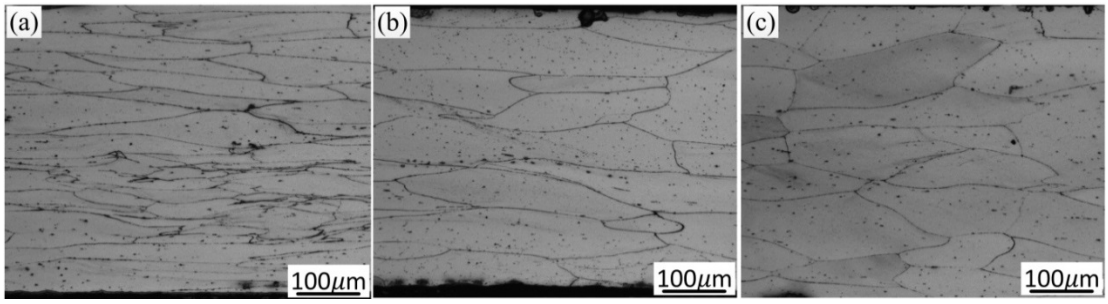

Figure 4. Microstructure of the warm-rolled sheets with hot rolling reduction of: (a) 40%; (b) 56%; (c) 68%.

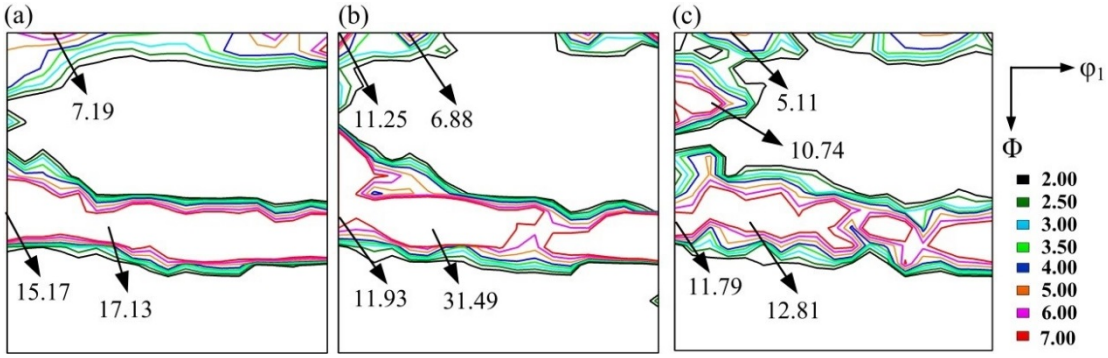

Figure 5. ODF (φ_2=45°) of the warm-rolled sheets with hot rolling reduction of: (a) 40%; (b) 56%; (c) 68%.

3.4. Microstructure and texture of the annealed sheets

Figure 6 shows the microstructure of the annealed sheets. It was found that the hot rolling reduction had an important role on the evolution of the final recrystallization microstructure. With the increase of hot rolling reduction, the average grain size of the annealed sheet was decreased at first and then increased. In the condition of 56% hot rolling reduction, the microstructural heterogeneity was the most obvious, as shown in Figure 6b. Figure 7 shows the texture of the annealed sheets. In the case of light hot rolling reduction (<56%), the texture was characterized by strong γ-fiber texture and weak α-fiber texture. The γ-fiber texture was reduced with the increase of rolling reduction. When the reduction reached 68%, the γ-fiber texture was weakest. It is interesting to note that strong γ-fiber texture was presented in the sample with 56% hot rolling reduction. As the reduction reached 68%, the final texture was more random, as shown in Figure 7c.

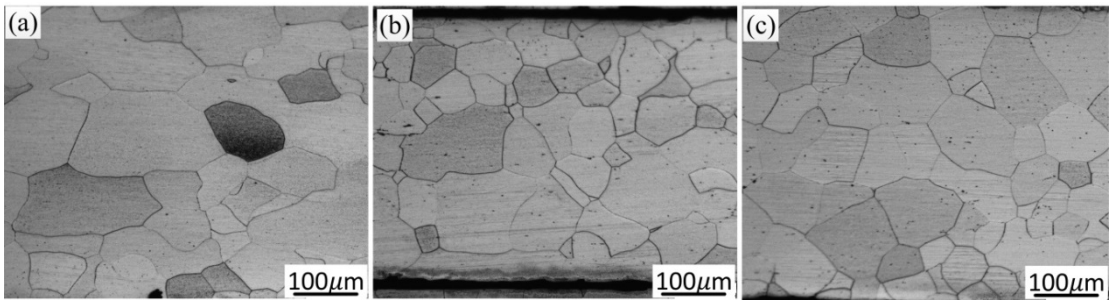

Figure 6. Microstructure of the annealed sheets with hot rolling reduction of: (a) 40%; (b) 56%; (c) 68%.

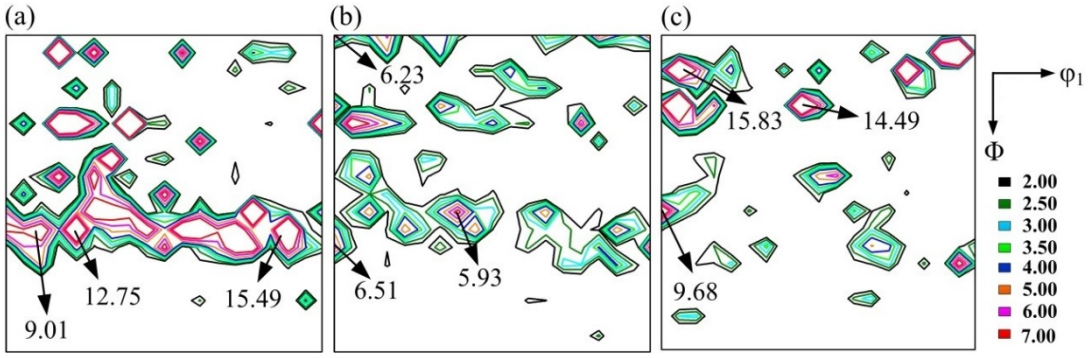

Figure 7. ODF (φ_2=45°) of the annealed sheets with hot rolling reduction of: (a) 40%; (b) 56%; (c) 68%.

3.5. Magnetic properties of the annealed sheets

Figure 8 show the magnetic properties of the final annealed sheets. It was found that the magnetic induction B_{50} increased at first and then decreased. As the reduction reached 56%, the magnetic induction B_{50} was 1.66 T. The magnetic induction B_8 without significant change decreased from 1.33 T to 1.31 T, as shown in the Figure 8a. The iron loss $P_{15/50}$ was reduced with increase in hot rolling reduction. As the reduction increased, however, the iron loss $P_{10/400}$ was decreased at first and then increased.

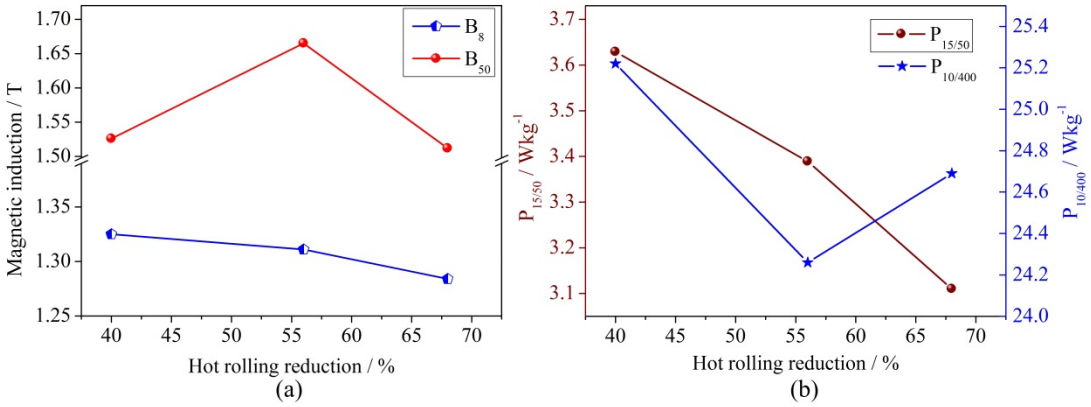

Figure 8. Magnetic properties of the annealed sheets: (a) magnetic induction; (b) iron loss.

4. Conclusions

It was found that the evolution of microstructure, texture and the magnetic properties highly depended on the hot rolling reduction. The initial as-cast strip was characterized by strong λ-fiber texture. The microstructure of hot rolled sheets was inhomogeneous. The λ-fiber texture decreased and the α-fiber, Goss texture increased with increasing hot rolling reduction. The warm-rolled texture was characterized by strong γ-fiber and weaker λ-fiber texture. After annealing, the texture of sample with 40% hot rolling reduction was dominated by strong γ-fiber, which was weakened with the increase in reduction. In addition, strong λ-fiber texture was developed in the sample with 56% hot rolling reduction. The magnetic induction B_{50} increased at first and then decreased, while the iron loss decreased at first and then increased. The highest B_{50} value attained was 1.66 T and the lowest $P_{10/400}$ was 24.26 W/kg at a reduction of 56%.

Acknowledgments
This work was financially supported by the National Natural Science Foundation of China (Nos.51674080, 51404155 and U1260204), the Program for New Century Excellent Talents in University (NCET-13-0111) and the Program for Liaoning Excellent Talents in University (LR2014007)。

References
[1] Roy R K, Panda A K, Ghosh M, Mitra A and Ghosh R N 2009 *J. Magn. Magn. Mater* **321** 2865-70
[2] Viala B, Degauque J, Baricco M, Ferrara E, Pasquale M and Fiorillo F 1996 *J. Magn. Magn. Mater*. **160** 315-7
[3] Kasama A H, Bolfarini C, Kiminami C S and Botta Filho W J 2007 *Mater. Sci. Eng. A* **449** 375-7
[4] Okada K, Yamaji T and Kasai K 1996 *ISIJ Int.* **36** 706-13
[5] Zapuskalov N 1999 *ISIJ Int.* **39** 463-70
[6] Li H Z, Liu H T, Liu Z Y, Lu H H, Song H Y and Wang G D 2014 *Mater. Charact.* **88** 1-6
[7] Liu H T, Li H Z, Li H L, Gao F, Liu G H, Luo Z H, Zhang F Q, Chen S L, Cao G M, Liu Z Y and Wang G D 2015 *J. Magn. Magn. Mater*. **391** 65-74
[8] Liu H T, Liu Z Y, Qiu Y Q, Sun Y and Wang G D 2012 J. *Mater Process.* Tec. **212** 1941-5
[9] Li H Z, Liu H T, Liu Z Y and Wang G D 2015 *Mater. Charact.* **103** 101-6
[10] Li H Z, Liu H T, Liu Y, Liu Z Y, Cao G M, Luo Z H, Zhang F Q, Chen S L, Lyu L and Wang G D 2014 *J. Magn. Magn. Mater*. **370** 6-12
[11] Li H Z, Liu Z Y 2015 *Mater. Sci. Eng. A* **639** 412-6